

Antibacterial activity of molybdenum disulfide and green silver nanoparticles reduced by tea tree essential oil compounds

Atividade antibacteriana de dissulfeto de molibdênio e nanopartículas de prata verde reduzida por compostos de óleo essencial de melaleuca

Actividad antibacteriana del disulfuro de molibdeno y nanopartículas de plata verde reducidas por compuestos de aceite esencial de melaleuca

Received: 05/08/2024 | Revised: 05/15/2024 | Accepted: 05/16/2024 | Published: 05/18/2024

Carlos Alves do Nascimento Filho

ORCID: <https://orcid.org/0000-0002-9237-3271>
Federal University of São Francisco Valley, Brazil
E-mail: carlosfilho85@hotmail.com

Fernando Antonio Gomes da Silva Jr

ORCID: <https://orcid.org/0000-0003-4096-8828>
Federal University of São Francisco Valley, Brazil
E-mail: nando.IF@hotmail.com

Mateus Matiuzzi da Costa

ORCID: <https://orcid.org/0000-0002-9884-2112>
Federal University of São Francisco Valley, Brazil
E-mail: mateus.costa@univasf.edu.br

Helinando Pequeno de Oliveira

ORCID: <https://orcid.org/0000-0002-7565-5576>
Federal University of São Francisco Valley, Brazil
E-mail: helinando.oliveira@univasf.edu.br

Abstract

The increasing resistance of microorganisms against antibiotics puts at risk the human being. This event requires urgently developing strategies for producing alternative antibacterial agents. The combination of green silver nanoparticles (reduced by essential oil) and molybdenum disulfide can be synergistically explored given the interaction of components. Herein, it is reported the response of isolated and combined components with resulting outstanding kinetics of kill-time (complete elimination of *Staphylococcus aureus* and *Escherichia coli* after four hours of contact), effective action against biofilm formation (~99% of inhibition in the biofilm formation). These results confirm that the intercalation of silver nanoparticles between exfoliated sheets of MoS₂ represents a promising strategy to develop efficient antibacterial agents against Gram-positive and Gram-negative bacteria.

Keywords: Tea tree; Silver nanoparticles; Molybdenum disulfide; Antibacterial.

Resumo

A crescente resistência dos microrganismos aos antibióticos coloca em risco o ser humano. Este evento requer o desenvolvimento urgente de estratégias para a produção de agentes antibacterianos alternativos. A combinação de nanopartículas de prata verde (reduzidas por óleo essencial) e dissulfeto de molibdênio pode ser explorada sinergicamente dada a interação dos componentes. Aqui, é relatada a resposta de componentes isolados e combinados com excelente cinética de tempo de morte (eliminação completa de *Staphylococcus aureus* e *Escherichia coli* após quatro horas de contato), ação eficaz contra a formação de biofilme (~99% de inibição no biofilme formação). Estes resultados confirmam que a intercalação de nanopartículas de prata entre folhas esfoliadas de MoS₂ representa uma estratégia promissora para desenvolver agentes antibacterianos eficientes contra bactérias Gram-positivas e Gram-negativas.

Palavras-chave: Melaleuca; Nanopartículas de prata; Dissulfeto de molibdênio; Antibacteriano.

Resumen

La creciente resistencia de los microorganismos frente a los antibióticos pone en riesgo al ser humano. Este evento requiere el desarrollo urgente de estrategias para la producción de agentes antibacterianos alternativos. La combinación de nanopartículas de plata verde (reducidas por aceite esencial) y disulfuro de molibdeno se puede explorar de forma sinérgica dada la interacción de los componentes. En este documento, se informa la respuesta de los componentes aislados y combinados con la resultante cinética sobresaliente de tiempo de muerte (eliminación completa de

Staphylococcus aureus y *Escherichia coli* después de cuatro horas de contacto), acción efectiva contra la formación de biopelículas (~99% de inhibición en la biopelícula formación). Estos resultados confirman que la intercalación de nanopartículas de plata entre láminas exfoliadas de MoS₂ representa una estrategia prometedora para desarrollar agentes antibacterianos eficientes contra bacterias Gram positivas y Gram negativas.

Palabras clave: Melaleuca; Nanopartículas de plata; Disulfuro de molibdeno; Antibacteriano.

1. Introduction

The prevalence of microorganisms in the presence of medications results from antimicrobial resistance (Dadgostar, 2019) in a process favored by the uncontrolled use of antibiotics in human and animal production (Levy, 2005; Levy, 1998). These antibiotic-resistant microorganisms lead to illness and prolonged hospital admission processes, considered a shadow epidemic due to the restricted treatment possibilities (Levy, 2005). This scenario is critical given the scarcity of new antibiotics (LEVY, 2005). Consequently, an intense effort has been observed to develop alternatives to control superbacteria proliferation.

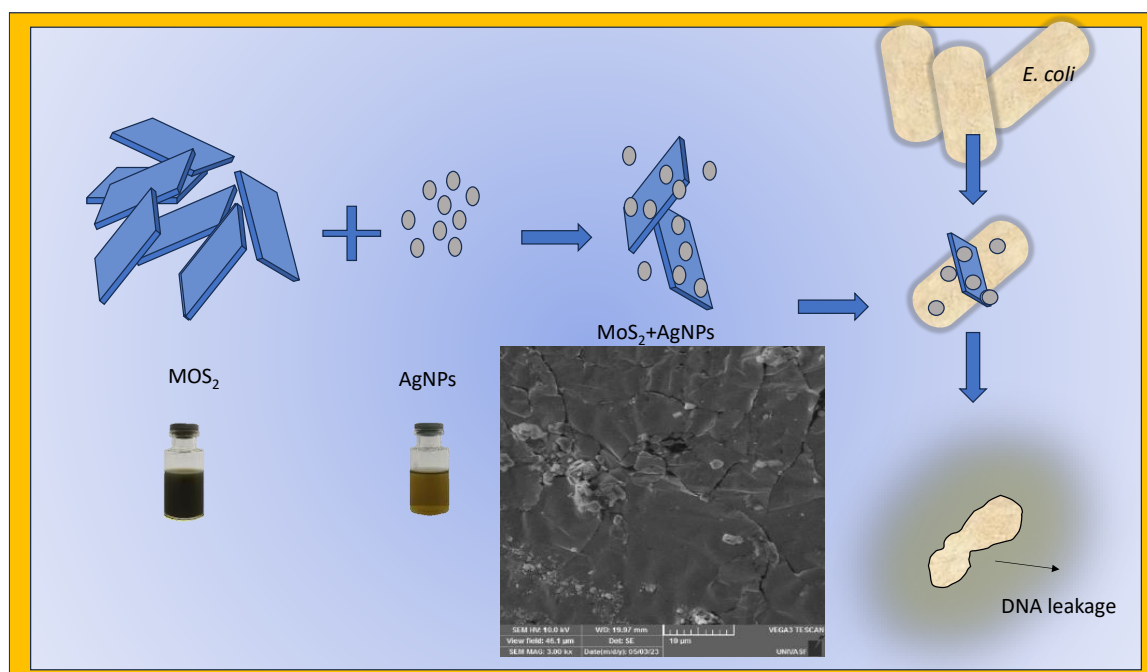
In particular, silver nanoparticles (Ag NPs) have been successfully applied as antibacterial agents in dermal wounds (Nam et al., 2015) and against a wide spectrum of bacterial species. The large surface area-volume ratio of metal nanoparticles improves the overall antibacterial activity of the resulting material (Yılmaz et al., 2023). The general mechanism involves a multifactor process that is based on the attachment of AgNPs to the cell membrane and the strong interaction with their sulfur and phosphate components (More et al., 2023), damaging their integrity by leakage of intracellular components (Bruna et al., 2021; Shaheen, 2016). Also, the formation of reactive oxygen species affects bacterial metabolism and DNA duplication (Shaheen, 2016).

An important aspect to be considered in the synthesis of silver nanoparticles is the environmental impact due to the use of toxic and harmful chemical agents (Vinicius de Oliveira Brisola Maciel et al., 2020). To circumvent these drawbacks, the green synthesis of silver nanoparticles has been considered an environmentally friendly process that considers the use of materials (such as extracts of plants and essential oils) that are rich in terpenes and flavonoids being relevant in the reduction of Ag⁺ to Ag⁰ (M.L. Guimarães et al., 2020; Milena Lima Guimarães et al., 2019, 2022a; Vinicius de Oliveira Brisola Maciel et al., 2020). Essential oils have been recognized by additional activities (antibacterial, antiviral, and antimycotic) that can be incorporated by the reduced nanoparticles (Milena Lima Guimarães & Amarante, 2021; Nehme et al., 2021).

On the other hand, MoS₂-based nanostructures have been successfully applied in the photothermal therapy of cancer, but also for antibacterial applications (Wentao Zhang et al., 2016). With this aim, the use of MoS₂ nanosheets has been considered in solar disinfection for multi-drug-resistant bacteria (Zhao et al., 2021) while the combination of MoS₂ and vancomycin has been applied in the photothermal treatment inhibiting the growth of *Staphylococcus aureus* (Weiwei Zhang et al., 2022).

Herein, green silver nanoparticles reduced by tea tree essential oil (melaleuca essential oil) are combined with molybdenum disulfide in composites that are applied as potential antibacterial agents against *S. aureus* and *E. coli* by exploring the combined action of essential oil as a reducing agent/ antibacterial component, silver nanoparticles and exfoliated sheets of molybdenum disulfide in a synergistic process that results in an efficient activity of bacterial inhibition at lower concentration of components. The response of composites of Ag/MoS₂ (isolated and combined) was evaluated from assays of agar diffusion, kill-time, biofilm inhibition, and toxicity. The general scheme with the aim of this paper is drawn in Figure 1, which represents the exfoliated sheets of MoS₂, the green silver nanoparticles (Ag NPs), and the composite (MoS₂+Ag NPs) – (with the corresponding SEM image of MoS₂ and aggregates of AgNPs) applied for adhesion on bacterial surface provoking the death of cells by leakage of vital fluids.

Figure 1 - General scheme for exfoliated nanosheets of MoS₂, silver nanoparticles, and MoS₂+Ag NPs nanostructures with the corresponding SEM image and the general process of nanoparticles adhesion and bacterial cell inactivation with DNA leakage.



Source: Authors

2. Methodology

Molybdenum disulfide (Radmax, Brazil), sodium hydroxide (Dinâmica, Brazil), ethyl alcohol (Dinâmica, Brazil), and silver nitrate (Aldrich, USA). Tryptic soybean broth (TSB) (Kasvi, Spain), phosphate buffered saline solution (PBS) (Kasvi, Spain), plate counter agar (PCA) AlphaTec (Brazil), and Brain Heart Infusion (BHI) (Kasvi, Spain) were used as received and all solutions were prepared using Milli-Q water. Tea tree essential oil (*Melaleuca alternifolia*) was purchased from Akã Oils Essential (Brazil).

Scanning Electron Microscope Vega 3XM, Tescan evaluated the morphology of materials. The absorbance in the UV-vis region was performed in a UV-vis Hach DR5000 using a single quartz cuvette in the range of 300 nm to 800 nm at a step of 1 nm. Zetasizer Nano ZS-90 Malvern provided data about the size of particles and zeta potential. FTIR Prestige-21 Shimadzu evaluated the structure of materials while the composition of MoS₂ was provided by an X-ray fluorescence spectrometer CTX model 800.

2.1 Exfoliation of Molybdenum disulfide

For exfoliation of molybdenum disulfide (Zhou et al., 2011), 120 mg of powder was dispersed in 30 mL of a solution containing 45% of ethanol and 55% of water with sodium hydroxide (10 mg) (Ikram et al., 2020) with the resulting solution sonicated for 8 hours. Subsequently, the samples were centrifuged at 15,000 rpm for 10 minutes. The resulting solution was dried and washed until it reached pH 7 providing the dispersion of MoS₂ nanosheets to be explored in the following synthesis of the MoS₂+AgNPs composite.

2.2 Synthesis of silver nanoparticles with exfoliated molybdenum disulfide

Silver nanoparticles were biosynthesized according to the method described by Maciel *et al.* (Maciel *et al.*, 2019) with some modifications. As a general standard method, an aliquot of tea tree oil (100 μL) was diluted in 17 mL of acetone at pH 8, which was adjusted by incorporating an aqueous NaOH solution (0.1 M). A second aqueous solution of silver nitrate (1 mM) was also prepared (system Ag NPs). For the preparation of MoS₂+Ag NPs, 30 mL of AgNO₃ received exfoliated MoS₂ nanosheets (from the reaction described in section 2.1), and it was kept under intense agitation and heating (95 °C). After this step, the tea tree oil solution was added dropwise into an aqueous silver nitrate solution with the MoS₂ nanosheets until it reached a total volume of 32 mL (2 mL of essential oil solution). The kinetics of silver nanoparticle formation associated with exfoliated molybdenum disulfide were monitored at fixed time intervals (15, 30, 45, and 60 min) with the measurement of the characteristic peak of absorbance of silver nanoparticles in the UV-Vis spectrum. All of the procedures were conducted in the dark to avoid the effect of light-induced degradation.

2.3 Broth microdilution assays

Broth microdilution assays were performed following the Institute for Clinical and Laboratory Standards (CLSI, 2019) for the determination of the minimum bactericidal concentration (MBC) of silver nanoparticle solutions prepared by green synthesis (Ag NPs system), MoS₂ system, and MoS₂ + AgNPs system. *S. aureus* (ATCC 25923) and *E. coli* (ATCC 25922) were kept in BHI at 4 °C until the use. Initially, 100 μL of TSB was added to each microplate well. Then, 100 μL of the solution under test (MoS₂, AgNPs, and MoS₂+AgNPs) were added to the first well and, after homogenization, it was transferred to the second well, and so on, obtaining concentrations of 1:1, 1:2, 1:4, 1: 8; 1:16; 1:32; 1:64; 1:128 compared to the initial concentration of the antibacterial agent and a bacterial suspension standardized to 0.5 McFarland scale was prepared. Aliquots of 10 μL were transferred to each well of the microplate containing the dilutions of the nanoparticle solutions, and incubated at 37 °C for 24 h. With the aid of a microplate replicator, an aliquot of the solution from the microplate wells was seeded on the surface of the PCA medium taken for 24 h at 37 °C.

2.4 Agar diffusion assays

The agar diffusion assays were performed according to Guimarães *et al.*, Gram-positive *S. aureus* (ATCC 25923) and gram-negative *E. coli* (ATCC 25922) bacterial inoculums were prepared from cultures maintained in agar at 4 °C. Then, aliquots of bacterial viable cells dispersed in culture media were removed and inserted into saline solution (0.85%), reaching turbidity of 0.5 on the McFarland scale (10⁸ CFU mL⁻¹). The bacterial suspension was distributed in a Petri dish containing PCA medium with a swab. Discs formed by liquid samples of MoS₂, AgNPs, and the MoS₂+AgNPs association were incorporated into the plates to assess their activity. After this step, the plate was incubated at 37 °C for 24 h (Milena Lima Guimarães *et al.*, 2022b).

2.5 Kill time assays

The shortest time for the samples to eliminate the bacteria from the medium was evaluated from kill time assays, using the bacterial inoculum *S. aureus* (ATCC 25923) and *E. coli* (ATCC 25922), which were prepared from cultures maintained in agar at 4 °C. Assays were performed as follows: 5 mL of 10⁸ CFU mL⁻¹ bacterial solution were placed in a test tube, which was further diluted to 10⁶ CFU mL⁻¹. After homogenizing the bacterial solution, the three samples (MoS₂, AgNPs, and MoS₂+AgNPs) were disposed of in three tubes. Positive control was performed to compare the results. Then, 100 μL aliquots were removed from the tubes at time intervals (1 h, 2 h, 3 h, and 4 h) and disposed of in Petri dishes containing PCA. The plates were kept at 37 °C for 24 hours (Milena Lima Guimarães *et al.*, 2022b).

2.6 Antibiofilm assays

Using a bacteriological loop, inoculums of *S. aureus* (ATCC 25923) and *E. coli* (ATCC 25922) were dispersed in 10 mL of TSB in different tubes. After preparing the bacterial solutions, the different compounds (MoS_2 , AgNPs, and MoS_2 +AgNPs) were added to three different tubes with the positive control performed for comparison with the results. Then, the tubes were incubated at 37 °C for 24 hours. After incubation, the contents of the tubes were discarded, the tubes were washed with milli-Q water and 12 mL of saline solution was added to each tube. Then, the tubes were sonicated in a bath ($f = 40$ kHz) for 15 min to remove the trapped species. Aliquots of 100 μL were taken in triplicate from each system and seeded in a PCA medium. After incubation at 37°C for 24 h, colonies were counted to determine the number of remaining viable cells in the biofilms.

2.7 Cytotoxicity assays

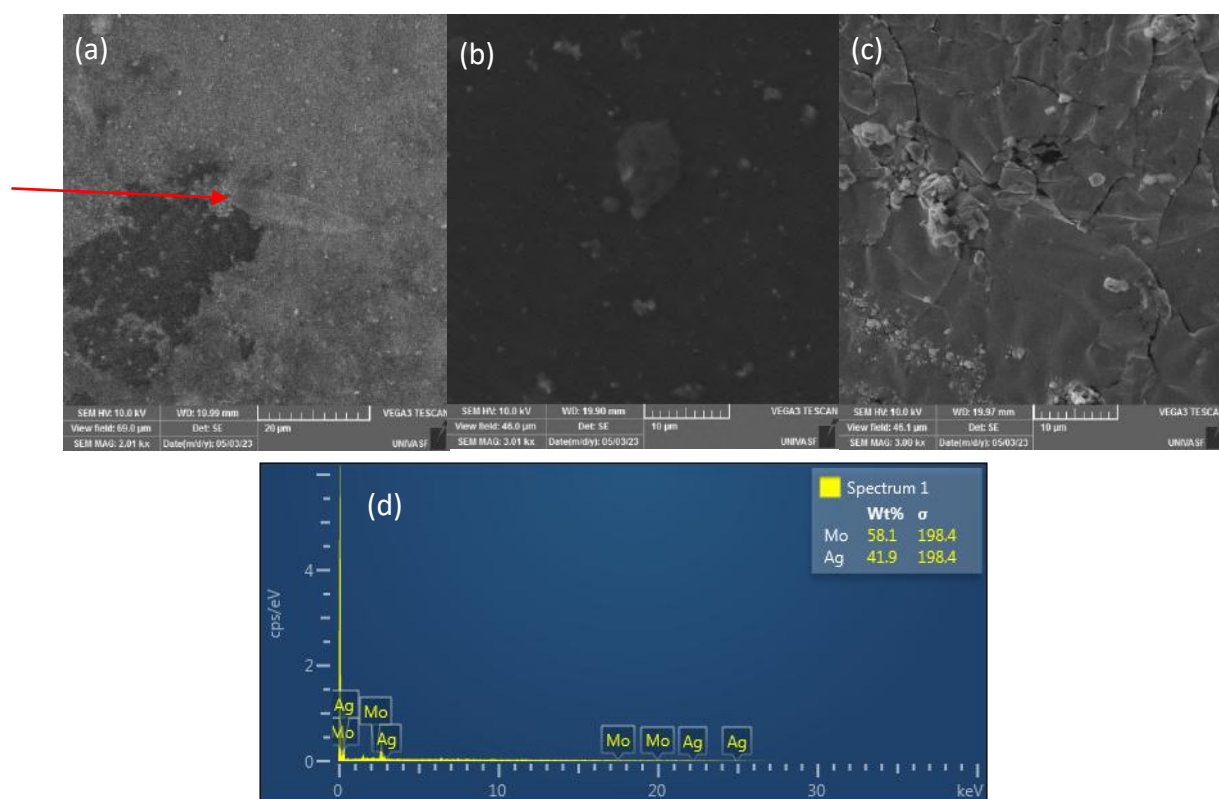
Dehydrated cysts of *Artemia salina* were purchased from a local aquarium store (Artemio Pur JBL GmbH&Co., Germany). Then, the cysts were hydrated in artificial seawater (ASA), dissolving 52.5 g of NaCl in 1.5 L of Milli-Q water under stirring (maintaining a concentration of 35 g/L) under artificial lighting (1500 lux supplied continuously by a fluorescent lamp). The nauplii hatched in 48 hours and after that period, the tests with the samples took place. Stock solutions of MoS_2 , AgNPs, and the MoS_2 +AgNPs systems were prepared and diluted in ASA, using the MBC value for each sample. 30 nauplii were placed in contact with each material under test in triplicate with the positive control applied for comparison (nauplii in artificial seawater). Suspensions diluted in ASA were vortexed and subsequently sonicated for 15 minutes to completely disperse the material under study.

The solutions were added to the 12-well plate, in triplicate. After that, 10 *Artemia Salina* nauplii were added to each well and incubated at 26 °C \pm 2 °C for 24 h. The number of surviving nauplii in each well was counted after 24 and 48 hours with larvae not fed in the bioassays. A nauplius is considered dead if there is no movement of its antennae after a slight agitation of the water for 10 seconds. Mortality percentages were calculated by comparing the number of survivors in the test and the control experiments.

3. Results and Discussion

Scanning electron microscopy images were performed to evaluate the morphology of MoS_2 , AgNPs, and the MoS_2 +AgNPs systems. As shown in Figure 2a, MoS_2 exhibits nanosheets-like morphology. Figure 2b shows silver nanoparticle aggregates for sample AgNPs, while sample MoS_2 +AgNPs shown in Figure 2c is characterized by a high density of sheets with intercalated and exfoliated structures with aggregates of silver nanoparticles on the molybdenum disulfide sheets. The components identification by the dispersive energy assays, by characteristic peaks of Mo and Ag (see Figure 2d) confirms the successful nucleation of silver nanoparticles in MoS_2 dispersion (Anderson et al., 2017).

Figure 2 - Scanning electron microscopy for (a) exfoliated molybdenum disulfide (b) silver nanoparticles (c) MoS₂+AgNPs and (d) EDS of the MoS₂+AgNPs sample.

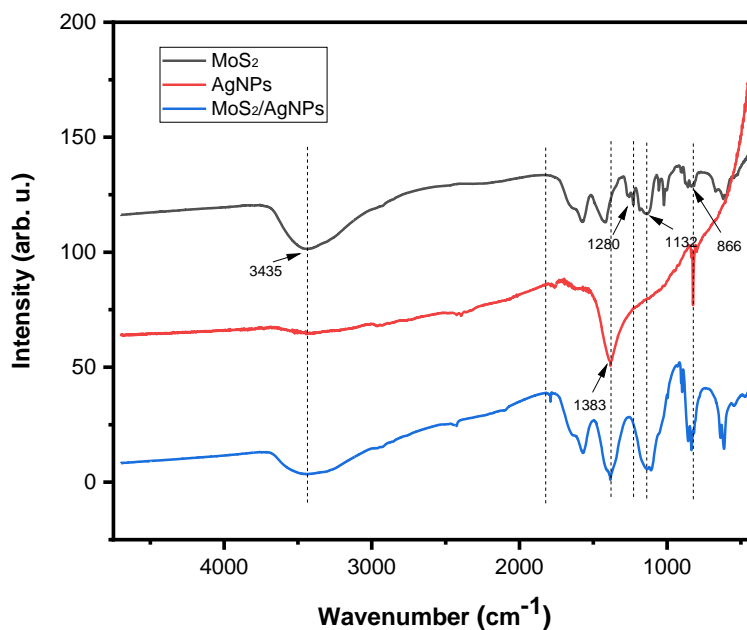


Source: Authors.

The evaluation of the composition of the molybdenum disulfide powder sample was scrutinized by using X-ray fluorescence spectroscopy. The result of the analysis indicates a content of Mo = 53.56%, S = 42.39%, SiO₂ = 5.92% and Fe = 1.49%. The characteristic groups of the samples MoS₂, Ag NPS, and MoS₂+AgNPs were studied by the FTIR spectrum, as summarized in Figure 3. As can be seen, the FTIR spectrum for molybdenum disulfide presents a strong absorption peak at 3435 cm⁻¹ due to the O-H stretching vibration (Awasthi et al., 2016) and a peak at 1132 cm⁻¹ attributed to the formation of sulfur complexes with the active sites of MoS₂ (Feng et al., 2014). The stretching vibrations of the C-O bond can be observed at 1228 cm⁻¹, which are groups resulting from the exfoliating solution (Bodík et al., 2019). The peak at 866 cm⁻¹ corresponds to the Mo-O elongation vibrations (Li et al., 2014), indicating that the exfoliated MoS₂ has partially oxidized edges (Ikram et al., 2020) while the band at 1019 cm⁻¹ is attributed to Mo-S vibrations (Ikram et al., 2020). The 1228 cm⁻¹ and 1130 cm⁻¹ bands correspond to SO₂ groups from interactions between sulfur from molybdenum disulfide and adsorbed oxygen (Bodík et al., 2019). The band around 878 cm⁻¹ represents the stretching vibration of the S-S bonds (Mohan et al., 2019).

The FTIR spectrum for the AgNPs shows a broad band at 3435 cm⁻¹ that is attributed to the O-H and N-H stretching vibrations. The band at 1383 cm⁻¹ arises from the C-O-H bending that can be attributed to polysaccharides commonly in plants (Bharadwaj et al., 2021; Huang et al., 2020). At 866 cm⁻¹, a band is attributed to the double bond between C=C carbon atoms, characteristic of essential oils. For the sample MoS₂+AgNPs, combined peaks are observed, confirming the presence of both components in the material.

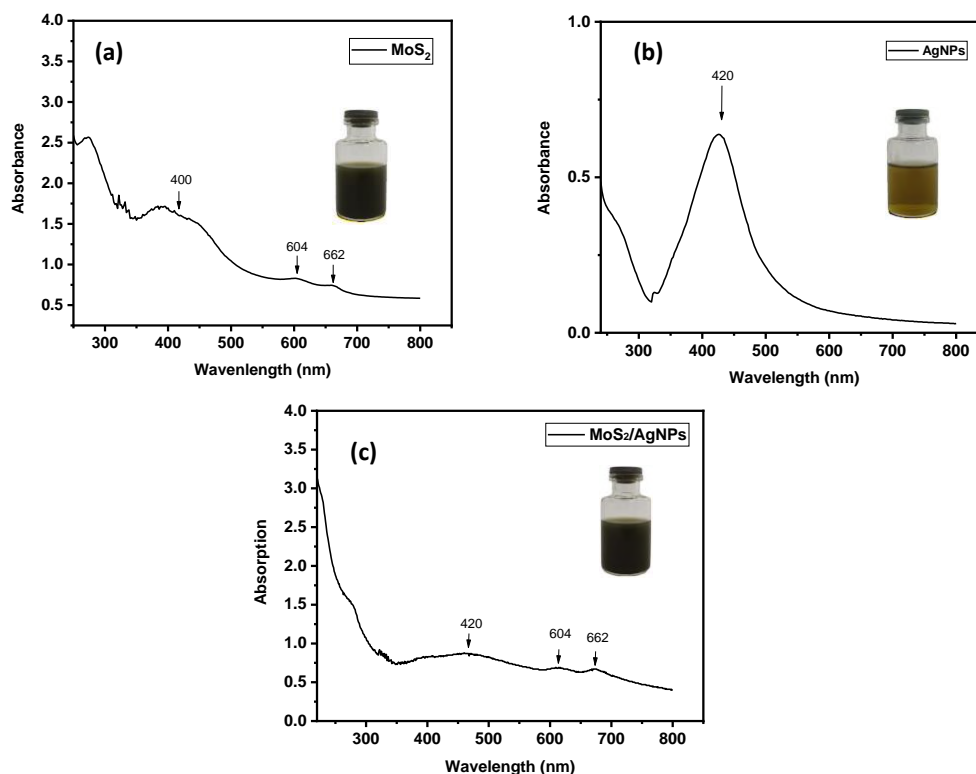
Figure 3 - FTIR spectrum for MoS₂ (curve in black), AgNPs (curve in red), and the MoS₂+AgNPs (curve in blue) samples.



Source: Authors.

The UV-Vis spectrum of the MoS₂ sample is shown in Figure 4a being characterized by bands centered at 604 nm and 662 nm, respectively (Winchester et al., 2014). These responses are characteristic of the 2H-MoS₂ phase (Eda et al., 2011). Also, a broad absorption peak at 400 nm confirms the theoretical and experimental values reported in the literature for MoS₂ (Mak et al., 2010).

Figure 4 - The UV-Vis spectrum of MoS₂ (a), Ag NPs (b), and MoS₂+ Ag NPs samples (c) with the corresponding photo of the resulting solution.



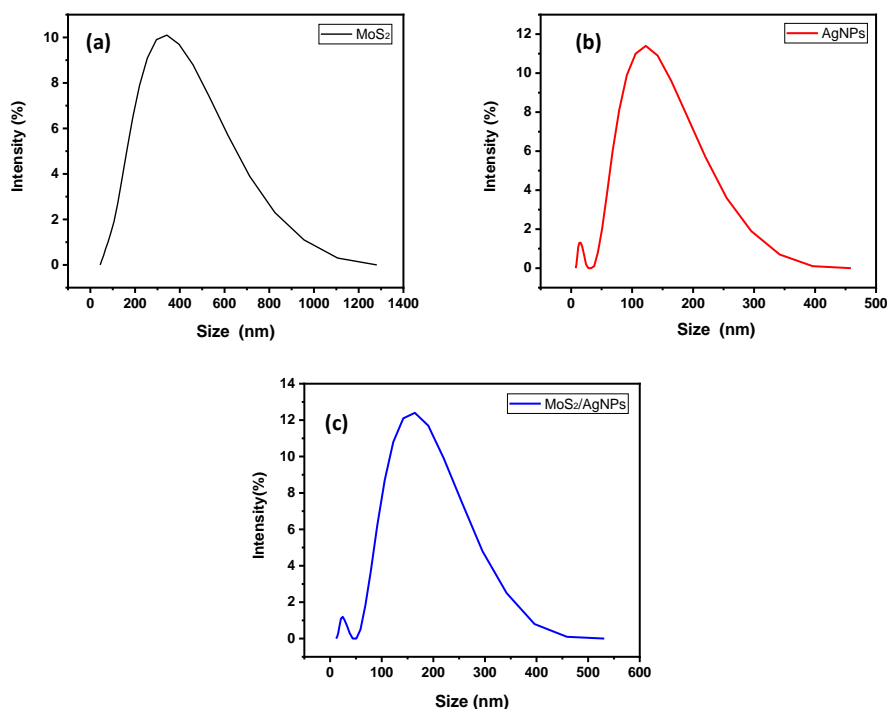
Source: Authors.

The optical response for nanoparticles synthesized from tea tree essential oil (Ag NPS system) is shown in Figure 4b. From this result, it is possible to observe an efficient activity of essential oil as reducing agents for silver ions from the observed plasmon band at 420 nm. The reduction of silver nanoparticles can be explained by the presence of monoterpenoids and biomolecules in an essential oil solution, described as potential silver ion reducers (Melo et al., 2020) in addition to α -pinene and γ -terpinene (Wei et al., 2020). The intensity at this peak position increases with reaction time, indicating progressive nucleation and formation of silver nanoparticles (Milena Lima Guimarães et al., 2021).

Figure 4c shows the UV-Vis absorption spectrum for the MoS₂+AgNPs system. As can be seen, there is a typical shift in the specific bands relative to MoS₂ and AgNPs samples, suggesting an additional step of aggregation level for these materials.

The size of particles is summarized in Figures. 5a, 5b and 5c for MoS₂, Ag NPs and MoS₂ +AgNPs compounds, respectively. As seen in Figure 5a, a single-size distribution is observed for exfoliated molybdenum disulfide, centered at 342 nm. For silver nanoparticles (see Figure 5b) two populations of size of particles are observed, at 15.69 nm and 122.4 nm. The presence of particles in the nanoscale is an important property to be considered in the applications as biomaterials for antibacterial application, improving their ability to attach to the bacterial cell wall (Agnihotri & Dhiman, 2017). The particle sizes for MoS₂ AgNPs compounds are characterized by particles at 24.36 nm and 164.2 nm, indicating that the exfoliation degree of MoS₂ is also affected by the intercalation of the AgNPs.

Figure 5 - Size distribution in (a) MoS₂, (b) Ag NPs, and (c) MoS₂+AgNPs systems.



Source: Authors.

The polydispersity index (PDI) is a dimensionless measurement of the particle size distribution, which ranges from 0 to 1. The smaller the PDI, the more homogeneous the sample. The sample MoS₂ presents a PDI of 0.255. The silver nanoparticles presented a PDI of 0.449, a less homogeneous distribution of particles. For sample MoS₂ + AgNPs, the PDI was 0.285. In addition, the system based on MoS₂ presented a zeta potential of -8.24 mV, the AgNPs presented a zeta potential of -2.48 mV and sample MoS₂+AgNPs presented a zeta potential of -7.80 mV, characterizing as experimental systems with low stability degree.

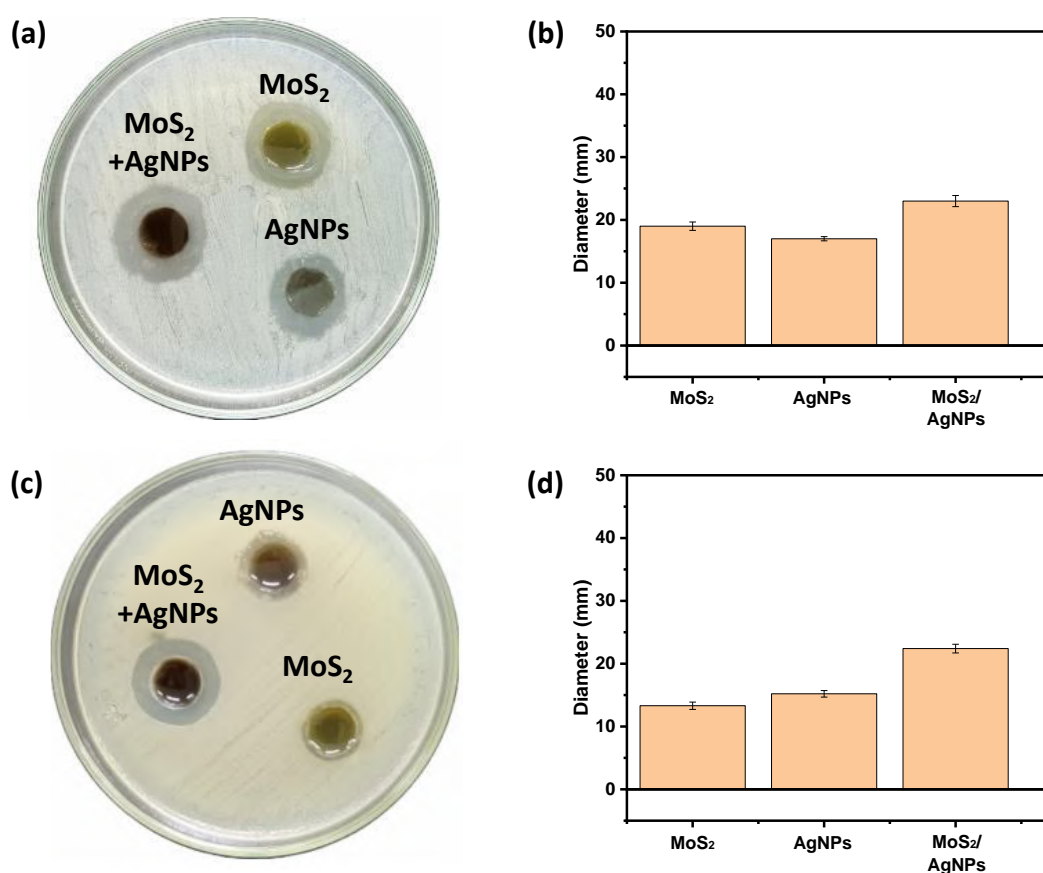
The broth microdilution test was applied in the MBC determination of different experimental systems against *S. aureus* (10⁶ CFU mL⁻¹) and *E. coli* (10⁶ CFU mL⁻¹). In a microplate, serial dilutions were made in the TSB broth of the c. Aliquots of 10 μ L of bacterial suspension were added to each well, except for wells applied as negative control (TSB solution). The results against *S. aureus* for MoS₂ samples returned efficiency at a dilution of 1:1. On the other hand, it was observed that silver nanoparticles obtained inhibition at a dilution of 1:4 and the sample MoS₂+AgNPs inhibited until a dilution of 1:16. For the system MoS₂, the complete elimination of bacteria was observed at a dilution of 1:2 while silver nanoparticles obtained inhibition at a dilution of 1:8 and for the system, MoS₂+AgNPs the value was reduced to 1:32.

As can be observed, with all of the dilution relative to the originally synthesized systems, the formulation MoS₂, AgNPs, and MoS₂+AgNPs were successfully applied against Gram-positive and Gram-negative bacteria with efficiency following the order MoS₂+ AgNPs > Ag NPs > MoS₂ with dilutions in the order of 1/32 from the initial concentration preserving antibacterial activity, an important advantage for this experimental system.

The agar diffusion tests were carried out for samples MoS₂, AgNPs, and MoS₂+AgNPs. The culture medium was placed in the Petri dish and then perforated to accommodate the solution under study with subsequent observation and identification of the inhibition halos of each material. The solutions were tested against *S. aureus* and *E. coli*. Figures 6a and 6b show the result of the inhibition halos against *S. aureus* while results in Figures 6c and 6d are observed for *E. coli*, in which it is possible to

observe increasing haloes for MoS₂, AgNPs, and MoS₂+AgNPs, in the following order: MoS₂ ~ AgNPs < MoS₂+AgNPs. The antibacterial activity observed for exfoliated molybdenum disulfide is attributed to the interaction of the edges of nanosheets with the bacterial membrane, resulting in cell damage and death.

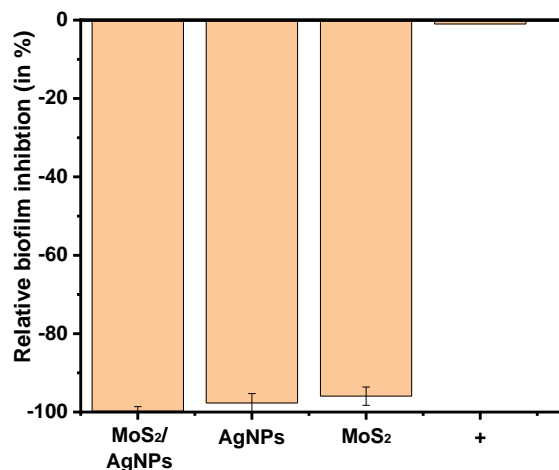
Figure 6 - Inhibition halo assay (a) and measured value for halo (b) for samples MoS₂, AgNPs, and MoS₂+AgNPs against *S. aureus* and inhibition halo assay (c) and measured value for halo (d) for samples MoS₂, AgNPs, and MoS₂+AgNPs against *E. coli*.



Source: Authors.

The antibiofilm activity of the compounds was evaluated from the direct count of viable cells attached to the reactor in contact. Figure 7 shows the result of antibiofilm activity against *S. aureus* (a typical biofilm-forming system) for the three different compositions. In biofilms, bacterial cells are encapsulated by secreted polymeric extracellular proteins that strongly protect bacterial cells from the effects of antibiotics. These results confirm the strong antibiofilm activity of materials in comparison with the control sample. For these compositions, an antibiofilm activity AB ~ 95% is observed for molybdenum disulfide nanosheets, AB ~ 97% for silver nanoparticles, and AB ~ 99% for the MoS₂+AgNPs system.

Figure 7 - Relative biofilm inhibition for exfoliated molybdenum disulfide, silver nanoparticles, and for the association between the two materials against *S. aureus*.

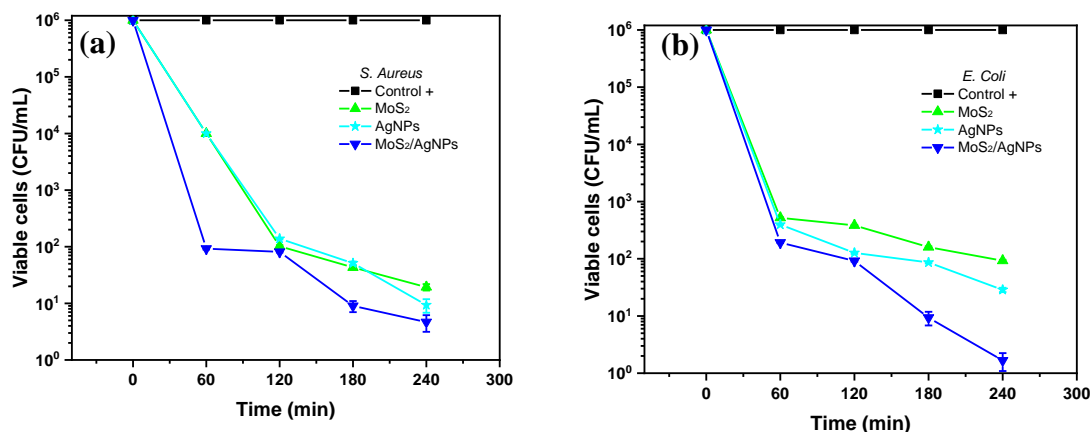


Source: Authors.

These results confirm the ability of exfoliated molybdenum disulfide, silver nanoparticles, and the association of the two materials to cross the extracellular polymeric matrix accessing the *S. aureus* viable cells embedded in the biofilm, causing membrane damage and death of cells (Roy et al., 2019). Thus, the ability of these materials to eradicate the biofilm of *S. aureus* opens the possibility to further explore these nanomaterials as a disinfection agent, with an improvement in the overall response for systems with the interaction of AgNPs and MoS₂.

The assays of the kinetics of death of bacteria (*S. aureus* and *E. coli*) provided by the three experimental systems (MoS₂, AgNPs, and MoS₂+AgNPs) were determined from the direct measurement of viable cells after fixed intervals of time of interaction of the bacteria with these three antibacterial agents. As can be seen in Figure 8, from a comparison of three experimental systems (against *S. aureus* (a) and *E. coli* (b)), the observed trend is a progressive reduction of viable bacteria with increasing treatment time, while the negative control (as expected) returned negligible variation in the number of viable cells for both bacteria.

Figure 8 - Kinetics of death time for different experimental systems against (a) *S. aureus* and (b) *E. coli* from the viable cell counts as a function of the reaction time induced by the action of MoS₂, AgNPs, and MoS₂+AgNPs in comparison with the control experiment.



Source: Authors.

As observed, a strong reduction in viable bacterial cells is observed in the first hour of the interaction. Throughout the experiments, a gradual and noticeable reducing number of viable bacterial cells is observed between 2h and 4h of the experiment. By direct comparison of the results, it is possible to verify that there is a synergism in the association between exfoliated molybdenum disulfide and silver nanoparticles, a fact that becomes from the evaluation of slope in the MoS₂+AgNPs system against the two bacterial strains. Intermediate performance is observed for silver nanoparticles and exfoliated molybdenum disulfide. A low percentage of immobilization (- 3.33%) was obtained for *Artemia Salina* nauplii treated with silver nanoparticles, 0% for molybdenum disulfide, and 0% for MoS₂+AgNPs system.

Accumulation of NPs on artemia was observed for all materials from a stereomicroscope equipped with a camera. Compared to the negative controls, it is possible to conclude that *Artemia* consumed the particles. The ingested particles appeared as a long dark streak within the bowels. This can be explained by the lack of food intake and absorption and the filling of the intestine with aggregates of nanoparticles. These results suggest that the silver nanoparticles synthesized by the green synthesis, the exfoliated molybdenum disulfide, and the association between these materials were not toxic to *Artemia Salina*.

4. Conclusion

Despite good performance against *S. aureus* and *E. coli* observed for individual components (AgNPs and MoS₂ samples), the combination of silver nanoparticles reduced by tea tree essential oil in the presence of molybdenum disulfide nanosheets demonstrated synergistic antibacterial performance with superior performance in terms of kinetics of inhibition, diffusive assays, and antibiofilm activity, in an indication that reduction of silver nanoparticles into exfoliated MoS₂ results in a material with intercalated nanosheets of MoS₂ decorated with silver nanoparticles that present economic advantages (reduction in the MBC), outstanding performance against biofilms and environmentally friendly component from the green synthesis of silver nanoparticles, being considered a promising new alternative for antibacterial system against Gram-positive and Gram-negative species. It is expected to develop novel prototypes based on adsorbing surfaces impregnated with MoS₂+AgNPs for application as smart and multifunctional cleaning fibers loaded with green-based compounds with mutual activity against planktonic and biofilm of single and multiple bacterial species.

Acknowledgments

This research was supported by Brazilian funding agencies CAPES, FINEP, FACEPE (APQ-0444-1.05/20), and CNPq.

References

- Agnihotri, S., & Dhiman, N. K. (2017). *Development of Nano-Antimicrobial Biomaterials for Biomedical Applications* (pp. 479–545). https://doi.org/10.1007/978-981-10-3328-5_12
- Anderson, K., Poulter, B., Dudgeon, J., Li, S.-E., & Ma, X. (2017). A Highly Sensitive Nonenzymatic Glucose Biosensor Based on the Regulatory Effect of Glucose on Electrochemical Behaviors of Colloidal Silver Nanoparticles on MoS₂. *Sensors*, *17*(8), 1807. <https://doi.org/10.3390/s17081807>
- Awasthi, G. P., Adhikari, S. P., Ko, S., Kim, H. J., Park, C. H., & Kim, C. S. (2016). Facile synthesis of ZnO flowers modified graphene like MoS₂ sheets for enhanced visible-light-driven photocatalytic activity and antibacterial properties. *Journal of Alloys and Compounds*, *682*, 208–215. <https://doi.org/10.1016/j.jallcom.2016.04.267>
- Bharadwaj, K. K., Rabha, B., Pati, S., Choudhury, B. K., Sarkar, T., Gogoi, S. K., Kakati, N., Baishya, D., Kari, Z. A., & Edinur, H. A. (2021). Green Synthesis of Silver Nanoparticles Using Diospyros malabarica Fruit Extract and Assessments of Their Antimicrobial, Anticancer and Catalytic Reduction of 4-Nitrophenol (4-NP). *Nanomaterials*, *11*(8), 1999. <https://doi.org/10.3390/nano11081999>
- Bodík, M., Annušová, A., Hagara, J., Mičušik, M., Omastová, M., Kotlár, M., Chlpík, J., Cirák, J., Švajdlenková, H., Anguš, M., Roldán, A. M., Veis, P., Jergel, M., Majkova, E., & Šiffalovič, P. (2019). An elevated concentration of MoS₂ lowers the efficacy of liquid-phase exfoliation and triggers the production of MoO_x nanoparticles. *Physical Chemistry Chemical Physics*, *21*(23), 12396–12405. <https://doi.org/10.1039/C9CP01951K>
- Bruna, T., Maldonado-Bravo, F., Jara, P., & Caro, N. (2021). Silver Nanoparticles and Their Antibacterial Applications. *International Journal of Molecular Sciences*, *22*(13), 7202. <https://doi.org/10.3390/ijms22137202>
- CLSI. (2019). Performance Standards for Antimicrobial Susceptibility Testing. 29th ed. CLSI supplement M100. *Performance Standards for Antimicrobial Susceptibility Testing. 29th Ed. CLSI Supplement M100*, 296.
- Dadgostar, P. (2019). Antimicrobial Resistance: Implications and Costs. *Infection and Drug Resistance*, *Volume 12*, 3903–3910. <https://doi.org/10.2147/IDR.S234610>
- Eda, G., Yamaguchi, H., Voiry, D., Fujita, T., Chen, M., & Chhowalla, M. (2011). Photoluminescence from Chemically Exfoliated MoS₂. *Nano Letters*, *11*(12), 5111–5116. <https://doi.org/10.1021/nl201874w>
- Feng, X., Xing, W., Song, L., & Hu, Y. (2014). In situ synthesis of a MoS₂/CoOOH hybrid by a facile wet chemical method and the catalytic oxidation of CO in epoxy resin during decomposition. *Journal of Materials Chemistry A*, *2*(33), 13299. <https://doi.org/10.1039/C4TA01885K>
- Guimarães, M.L., da Silva, F. A. G., da Costa, M. M., & de Oliveira, H. P. (2020). Green synthesis of silver nanoparticles using Ziziphus joazeiro leaf extract for production of antibacterial agents. *Applied Nanoscience (Switzerland)*, *10*(4). <https://doi.org/10.1007/s13204-019-01181-4>
- Guimarães, Milena Lima, & Amarante, J. F. (2021). *A importância dos óleos essenciais na síntese verde de nanopartículas metálicas The importance of essential oils in the green synthesis of metallic nanoparticles.*
- Guimarães, Milena Lima, Amarante, J. F., & Oliveira, H. P. de. (2021). A importância dos óleos essenciais na síntese verde de nanopartículas metálicas. *Matéria (Rio de Janeiro)*, *26*(3). <https://doi.org/10.1590/s1517-707620210003.13053>
- Guimarães, Milena Lima, da Silva, F. A. G., de Souza, A. M., da Costa, M. M., & de Oliveira, H. P. (2022a). All-green wound dressing prototype based on Nile tilapia skin impregnated with silver nanoparticles reduced by essential oil. *Applied Nanoscience*, *12*(2), 129–138. <https://doi.org/10.1007/s13204-021-02249-w>
- Guimarães, Milena Lima, da Silva, F. A. G., de Souza, A. M., da Costa, M. M., & de Oliveira, H. P. (2022b). All-green wound dressing prototype based on Nile tilapia skin impregnated with silver nanoparticles reduced by essential oil. *Applied Nanoscience 2021 12:2*, *12*(2), 129–138. <https://doi.org/10.1007/S13204-021-02249-W>
- Guimarães, Milena Lima, Silva Jr, F. A. G., Costa, M. M., & Oliveira, H. P. (2019). Green synthesis of silver nanoparticles using Ziziphus joazeiro leaf extract for production of antibacterial agents. *Applied Nanoscience*, *0123456789*. <https://doi.org/10.1007/s13204-019-01181-4>
- Huang, W., Nie, Y., Zhu, N., Yang, Y., Zhu, C., Ji, M., Wu, D., & Chen, K. (2020). Hybrid Label-Free Molecular Microscopies for Simultaneous Visualization of Changes in Cell Wall Polysaccharides of Peach at Single- and Multiple-Cell Levels during Postharvest Storage. *Cells*, *9*(3), 761. <https://doi.org/10.3390/cells9030761>
- Ikram, M., Tabassum, R., Kumar, U., Ali, S., Ul-Hamid, A., Haider, A., Raza, A., Imran, M., & Ali, S. (2020). Promising performance of chemically exfoliated Zr-doped MoS₂ nanosheets for catalytic and antibacterial applications. *RSC Advances*, *10*(35), 20559–20571. <https://doi.org/10.1039/D0RA02458A>
- LEVY, S. (2005). Antibiotic resistance—the problem intensifies. *Advanced Drug Delivery Reviews*, *57*(10), 1446–1450. <https://doi.org/10.1016/j.addr.2005.04.001>
- Levy, S. B. (1998). The Challenge of Antibiotic Resistance. *Scientific American*, *278*(3), 46–53. <https://doi.org/10.1038/scientificamerican0398-46>
- Li, J., Tang, W., Yang, H., Dong, Z., Huang, J., Li, S., Wang, J., Jin, J., & Ma, J. (2014). Enhanced electrocatalytic activity of Ni_{1-x}Fe_x alloy supported on polyethyleneimine functionalized MoS₂ nanosheets for hydrazine oxidation. *RSC Adv.*, *4*(4), 1988–1995. <https://doi.org/10.1039/C3RA42757A>

- Maciel, M. V. de O., Almeida, A. da R., Machado, M. H., Melo, A. P. Z., Rosa, C. G. da, Freitas, D. Z., Noronha, Carolina Montanheiro Teixeira, G. L., Armas, R. D., & Barreto, P. L. M. (2019). *Syzygium aromaticum* L. (Clove) Essential Oil as a Reducing Agent for the Green Synthesis of Silver Nanoparticles. *Open Journal of Applied Sciences*, 45–54. <https://doi.org/10.4236/ojapps.2019.92005>
- Mak, K. F., Lee, C., Hone, J., Shan, J., & Heinz, T. F. (2010). Atomically Thin MoS_2 : A New Direct-Gap Semiconductor. *Physical Review Letters*, 105(13), 136805. <https://doi.org/10.1103/PhysRevLett.105.136805>
- Melo, A. P. Z., Maciel, M. V. de O. B., Sganzerla, W. G., Almeida, A. de R., Armas, R. D., Machado, M. H., Rosa, C. G., Nunes, R. M., Bertoldi, F. C. B., & Barreto, P. L. M. (2020). Antibacterial activity, morphology, and physicochemical stability of biosynthesized silver nanoparticles using thyme (*Thymus vulgaris*) essential oil. *Materials Research Express*, 015087. <https://doi.org/10.1088/2053-1591/ab6c63>
- Mohan, M., Unni, K. N. N., & Rakhi, R. B. (2019). 2D organic-inorganic hybrid composite material as a high-performance supercapacitor electrode. *Vacuum*, 166, 335–340. <https://doi.org/10.1016/j.vacuum.2018.10.051>
- More, P. R., Pandit, S., Filippis, A. De, Franci, G., Mijakovic, I., & Galdiero, M. (2023). Silver Nanoparticles: Bactericidal and Mechanistic Approach against Drug Resistant Pathogens. *Microorganisms*, 11(2), 369. <https://doi.org/10.3390/microorganisms11020369>
- Nam, G., Rangasamy, S., Purushothaman, B., & Song, J. M. (2015). The Application of Bactericidal Silver Nanoparticles in Wound Treatment. *Nanomaterials and Nanotechnology*, 5, 23. <https://doi.org/10.5772/60918>
- Nehme, R., Andrés, S., Pereira, R. B., Ben Jemaa, M., Bouhallab, S., Ceciliani, F., López, S., Rahali, F. Z., Ksouri, R., Pereira, D. M., & Abdennebi-Najar, L. (2021). Essential Oils in Livestock: From Health to Food Quality. *Antioxidants*, 10(2), 330. <https://doi.org/10.3390/antiox10020330>
- Roy, S., Mondal, A., Yadav, V., Sarkar, A., Banerjee, R., Sanpui, P., & Jaiswal, A. (2019). Mechanistic Insight into the Antibacterial Activity of Chitosan Exfoliated MoS_2 Nanosheets: Membrane Damage, Metabolic Inactivation, and Oxidative Stress. *ACS Applied Bio Materials*, 2(7), 2738–2755. <https://doi.org/10.1021/acsabm.9b00124>
- Shaheen, H. M. (2016). Wound healing and silver nanoparticles. *Global Drugs and Therapeutics*, 1(1). <https://doi.org/10.15761/GDT.1000105>
- Vinicius de Oliveira Brisola Maciel, M., da Rosa Almeida, A., Machado, M. H., Elias, W. C., Gonçalves da Rosa, C., Teixeira, G. L., Noronha, C. M., Bertoldi, F. C., Nunes, M. R., Dutra de Armas, R., & Manique Barreto, P. L. (2020). Green synthesis, characteristics and antimicrobial activity of silver nanoparticles mediated by essential oils as reducing agents. *Biocatalysis and Agricultural Biotechnology*, 28, 101746. <https://doi.org/10.1016/j.bcab.2020.101746>
- Wei, C., Ma, Z., Qiao, J., Lin, J., & Li, G. (2020). Effects of different drying methods on volatile composition of *Melaleuca alternifolia* essential oil. *IOP Conference Series: Earth and Environmental Science*, 559(1), 012010. <https://doi.org/10.1088/1755-1315/559/1/012010>
- Winchester, A., Ghosh, S., Feng, S., Elias, A. L., Mallouk, T., Terrones, M., & Talapatra, S. (2014). Electrochemical Characterization of Liquid Phase Exfoliated Two-Dimensional Layers of Molybdenum Disulfide. *ACS Applied Materials & Interfaces*, 6(3), 2125–2130. <https://doi.org/10.1021/am4051316>
- Yılmaz, G. E., Göktürk, I., Ovezova, M., Yılmaz, F., Kılıç, S., & Denizli, A. (2023). Antimicrobial Nanomaterials: A Review. *Hygiene*, 3(3), 269–290. <https://doi.org/10.3390/hygiene3030020>
- Zhang, Weiwei, Kuang, Z., Song, P., Li, W., Gui, L., Tang, C., Tao, Y., Ge, F., & Zhu, L. (2022). Synthesis of a Two-Dimensional Molybdenum Disulfide Nanosheet and Ultrasensitive Trapping of *Staphylococcus Aureus* for Enhanced Photothermal and Antibacterial Wound-Healing Therapy. *Nanomaterials*, 12(11), 1865. <https://doi.org/10.3390/nano12111865>
- Zhang, Wentao, Shi, S., Wang, Y., Yu, S., Zhu, W., Zhang, X., Zhang, D., Yang, B., Wang, X., & Wang, J. (2016). Versatile molybdenum disulfide based antibacterial composites for in vitro enhanced sterilization and in vivo focal infection therapy. *Nanoscale*, 8(22), 11642–11648. <https://doi.org/10.1039/C6NR01243D>
- Zhao, Y., Jia, Y., Xu, J., Han, L., He, F., & Jiang, X. (2021). The antibacterial activities of MoS_2 nanosheets towards multi-drug resistant bacteria. *Chemical Communications*, 57(24), 2998–3001. <https://doi.org/10.1039/D1CC00327E>
- Zhou, K.-G., Mao, N.-N., Wang, H.-X., Peng, Y., & Zhang, H.-L. (2011). A Mixed-Solvent Strategy for Efficient Exfoliation of Inorganic Graphene Analogues. *Angewandte Chemie International Edition*, 50(46), 10839–10842. <https://doi.org/10.1002/anie.201105364>